Detection of Small Changes in Power Systems with Hardware-in-Loop Testing

Sanjay Hosur and Dongliang Duan

***Abstract*—In this paper, the subspace based output only detection algorithm proposed in our previous work [1]–[3] is applied to detect small changes in power systems. In this work, the disturbances considered are the ones that cause the operating point of power systems to change gradually or subtly over time, which are difficult to be captured by most existing detection tools. The simulation is carried out using the Opal-RT Real Time Digital Simulator (RTDS). The IEEE 39-bus system is simulated with this hardware in the loop testing platform. The changes studied are slow load rampings in the system. Results show that these small changes can be well detected by our algorithm.**

I. Introduction

In this paper the algorithm proposed in our previous work [1]–[3] will be tested. Our previous work demonstrated the algorithm can successfully detect system operating point. The algorithm has been applied to the detection of various events such as forced oscillations, the topology changes of the system, the ringdown events and so on. The focus of this work is to evaluate the response of the proposed detection algorithm to subtle and gradual changes such as the ramping events. The testing is done by combining two major research topics namely ramping events and hardware-in-the-loop testing for which a brief introduction of each topic is given below.

A. Ramping Events

There is a lot of emphasis on integrating the renewable energy sources with the existing power grid. The uncertainty associated with the these energy sources present the researchers with many new challenges as the power system operators strive to operate the grid in a reliable, secure and economically efficient way [4]–[6]. Of these one of the major challenges is the ramping events which are caused by fluctuation with varying magnitudes and durations.

Ramping events occur in wind power generation and possible causes include thunderstorms, wind gusts, and cyclones. Solar power ramping might be caused by short term microclimates like passing of a cloud. Load ramping events will generally be caused by human behavior. Generally the load ramping is more stable compared with the renewable sources of energy [5].

The renewable energy plant sites cannot be predetermined in the same way as the conventional energy generation plant sites. The arbitrary development of renewable energy sources can unexpectedly change the traditional grid load profile and operational practices [7] which demands a more situational awareness. The situational awareness can be achieved with quick and accurate detection of even the smallest changes in the system operating point.

Sanjay Hosur and Dongliang Duan are with the Department of Electrical and Computer Engineering at the University of Wyoming, Laramie, WY 820781. Emails: shosur@uwyo.edu, dduan@uwyo.edu.

This work was in part supported by the Department of Energy under grant DE-SC0012671 and the National Science Foundation under awards ECCS-1828066 and OAC-1923983.

B. Hardware-in-the-Loop Testing

The hardware in the loop (HIL) testing concept has been around for at least last five decades [8]. In [9] the authors define HIL testing. They have also introduced the advantages of having a HIL simulation in the design and testing of the control hardware and software. Testings can now be done without having to operate a real process and under imaginable extreme conditions in the laboratory environment.

HIL testing has been used in various fields such as flight simulation, missile guidance system, anti-lock braking system. to name a few. For power systems, HIL testing has also been applied to test different scenarios. Examples include unified testing platform for wind energy system [10], operation and control function of micro grid [11], photo voltaic control systems [12] and so on.

The significance of HIL testing has been recognized very well. Therefore, a benchmark for testing the distributed energy sources using HIL testing was published in 2018 [13]. It focused on benchmarking two test setups for control HIL (CHIL) and power HIL (PHIL) testing with recommendations on the equipment and reference laboratory procedures.

In this paper, HIL testing is incorporated to take advantage of the fact that the simulations can be carried out in real time. Various scenarios can be generated even for the cases where the data from real world is not available.

The rest of the paper is organized as follows. Section II gives a brief overview of the subspace based output only change point detection algorithm. Section III describes the HIL test setup. Section IV first discusses the results based on a simple system and next on the IEEE 39-bus system which uses the HIL test setup described. Section V draws some conclusions and highlights the future work to be done.

II. The Detection Algorithm [3]

The basic idea of the detection algorithm is discussed in papers [1], [2]. The enhancement of the algorithm with a statistical method called cumulative sum (CUSUM) is discussed in [3]. Here a very brief summary of the algorithm is presented.

2021 IEEE Power & Energy Society General Meeting (PESGM) | 978-1-6654-0507-2/21/$31.00 ©2021 IEEE | DOI: 10.1109/PESGM46819.2021.9637887

978-1-6654-0507-2/21/$31.00 ©2021 IEEE

In general, the dynamic model for a discrete-time system can be given by

$$\begin{aligned} \boldsymbol{x}_{k+1} &= \boldsymbol{F}\boldsymbol{x}_k + \boldsymbol{\epsilon}_k \\ \boldsymbol{y}_k &= \boldsymbol{H}\boldsymbol{x}_k + \boldsymbol{\nu}_k \ , \end{aligned} \tag{1}$$

where $\boldsymbol{x}$ is the state vector of size $m \times 1$, $\boldsymbol{y}$ is the observation/output vector of size $n \times 1$, $\boldsymbol{F}$ is the state transition matrix of size $m \times m$, $\boldsymbol{H}$ is the observation matrix of size $n \times m$, $\boldsymbol{\epsilon}_k$ and $\boldsymbol{\nu}_k$ are system input ($m \times 1$) and measurement noise ($n \times 1$) respectively. In general, for any system, the measurement noise can treated as additive white Gaussian noise. In the context of power systems, $\boldsymbol{\epsilon}_k$ is modeling the random load variations, which can be represented by a white Gaussian noise. After $\boldsymbol{\epsilon}_k$ passes through the system represented by Eq. (1), the output or the observation $\boldsymbol{y}_k$ will be a colored noise.

A. Subspace-Driven Output-Only Based Change-Point Detection

The output-only covariance-based subspace system identification is based upon the the auto-covariance of the output $\boldsymbol{y}_k$: (see e.g. [14]–[17])

$$R_i = \mathbb{E}(\boldsymbol{y}_k^T \boldsymbol{y}_{k-i}) \ . \tag{2}$$

The Hankel matrix using the auto-covariance of the output defines the signal space and is given by

$$\mathcal{H}_{p+1,q} = \text{Hank}(R_i) = \begin{bmatrix} R_0 & R_1 & R_2 & \dots & R_{q-1} \\ R_1 & R_2 & \ddots & \ddots & R_q \\ \vdots & \vdots & \ddots & \ddots & \vdots \\ R_p & R_{p+1} & \dots & \dots & R_{p+q-1} \end{bmatrix} ,$$

where p and q are the model order used in the subspace identification method. Defining the orthogonal matrix $\mathcal{U}$ such that

$$\mathcal{U}^T\mathcal{U} = \boldsymbol{I} \ \text{ and } \ \mathcal{U}^T\mathcal{H}_{p+1} = \boldsymbol{0} \ . \tag{3}$$

The matrix $\mathcal{U}$ is not unique, but when the signal space remains unchanged, then the following equation holds,

$$\mathcal{U}\mathcal{H}_{p+1,q} = \boldsymbol{0} \ . \tag{4}$$

The matrix $\mathcal{U}$ can be also called the "null space" of the signal. Eq. (4) holds only theoretically. In practice, the exact Hankel matrix $\mathcal{H}_{p+1,q}$ is not obtainable and can only be estimated from some available observation data as $\hat{\mathcal{H}}_{p+1,q}$ via replacing the expectation by the sample average. For each N-point observation window starting at time n, we can define a residue as

$$\boldsymbol{\zeta}(n) = \hat{\mathcal{U}}\hat{\mathcal{H}}_{p+1,q}(n) \ . \tag{5}$$

B. The CUSUM Procedure

The residue derived above in Eq. (5) is extended here to develop the CUSUM strategy [14], [16], [17]. This residue is expected to have zero mean with a normal distribution by the central limit theorem. The detailed derivation can be found in [3]. A summary of the equations used is given here.

Let μ_0 be the mean before change and μ_1 after change with $\mu_0 < \mu_1$. Suppose the mean changes at time r, then the change in mean can be represented as

$$\mu_n = \begin{cases} \mu_0, & \text{if } n \le r-1 \\ \mu_1, & \text{if } n \ge r \ . \end{cases} \tag{6}$$

The problem is to detect the change in the mean μ_n and estimate the change time r. The detection problem is basically the testing between the hypotheses

$$\begin{aligned} H_0 &: r > n \\ H_1 &: r \le n \ . \end{aligned} \tag{7}$$

Taking the likelihood ratio between the two hypothesis and assuming Gaussian distribution, the maximum likelihood estimate of unknown jump time r under H_1 is

$$\arg \max_{1 \le r \le n} S_r^n(\mu_0, \nu) \ , \tag{8}$$

where $\nu = \mu_1 - \mu_0$. Then the detector can be defined as

$$g_n \overset{\text{def}}{=} \Lambda_n(\hat{r}_n) = \max_r S_r^n(\mu_0, \nu) \underset{H_0}{\overset{H_1}{\gtrless}} \lambda \ , \tag{9}$$

where λ is the threshold and the detector in recursive form is

$$g_n = (g_{n-1} + y_n - \mu_0 - \frac{\nu}{2})^+ \ . \tag{10}$$

The $^+$ sign indicates that mean after change is greater than mean before change (i.e., $\mu_0 < \mu_1$).

In practice, it is not always possible to know the mean μ_1 after the change, especially in the case of on-line testing. Thus, two tests are run in parallel with ν being replaced with minimum jump magnitude v_m that is chosen *a priori*. One test will be checking for an increase in mean while the second test will be checking for a decrease in mean. The stopping rules can be defined as:

When the mean **increases** after the change:

$$\begin{cases} U_0 = 0 & \text{(11a)} \\ U_n = \sum_{k=1}^{n} (y_n - \mu_0 - \frac{v_m}{2}) & \text{(11b)} \\ m_n = \min_{0 \le k \le n} U_k & \text{(11c)} \\ g_n^+ \overset{\text{def}}{=} U_n - m_n & \text{(11d)} \\ \text{alarm when } g_n^+ > \lambda & \text{(11e)} \end{cases}$$

When the mean **decreases** after the change:

$$\begin{cases} T_0 = 0 & \text{(12a)} \\ T_n = \sum_{k=1}^{n} (y_n - \mu_0 + \frac{v_m}{2}) & \text{(12b)} \\ M_n = \max_{0 \le k \le n} T_k & \text{(12c)} \\ g_n^- \overset{\text{def}}{=} M_n - T_n & \text{(12d)} \\ \text{alarm when } g_n^- > \lambda & \text{(12e)} \end{cases}$$

where λ is the threshold.

The first rule to stop makes the decision and the jump time n is estimated by last maximum (or minimum respectively) time

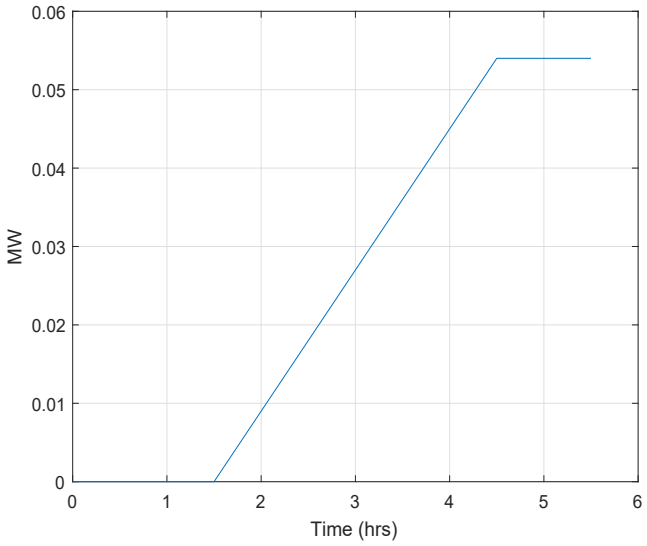

Fig. 1. The load profile.

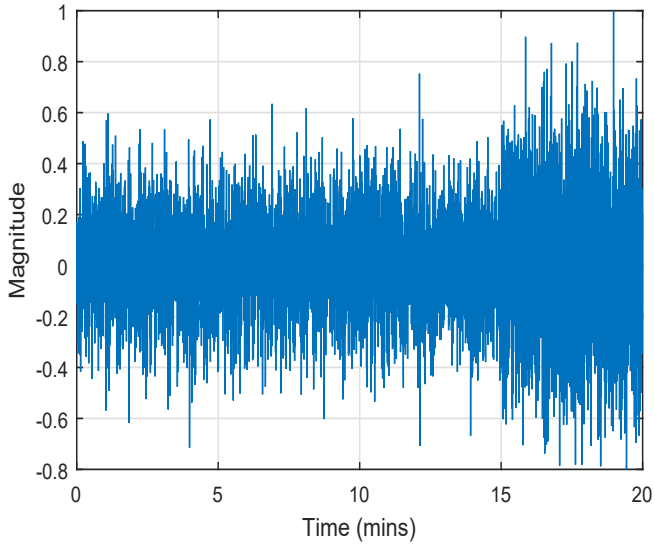

Fig. 2. The output of simulation of the simplified model.

before detection. Eqs. (11b) and (12b) represent the CUSUM statistics and Eqs. (11c) and (12c) represents the extremes. The Eq. (11d) and Eq. (12d) represent the CUSUM decision statistics. The decision statistics will be zero until a change is detected.

III. Hardware-in-the-Loop Setup

The standard IEEE 39-bus power system is simulated on the Opal-RT Real Time Digital simulator (RTDS). The load is varied externally and given as an input to the simulated system. For simulation, the system model is built in simulink. Using the RT-Lab software, which is a proprietary software of Opal-RT, the modeled system is compiled and run on the RTDS.

For the case presented here the phasor data was written into a file and the detection algorithm was tested offline. The Opal-RT RTDS is a powerful simulator with multiple cores and several simulators can be interfaced together for one simulation. This setup will help create a more realistic testing model as the algorithm can be tested online while the network latency and other parameters can mimic the real-world scenario more closely.

The total simulation time is 5.5 hours. The load ramping starts at 1.5 hours and ramped up till 4.5 hours. The load connected to bus 20 of the simulated system is ramped up. The ramp has a slope of 5×10^{-6} as we want to see the behavior of algorithm for small changes. The data is collected at 100 samples/second and down sampled to 5 samples/second. The data from 30 mins to 1 hour is used for null space estimation. The algorithm is run from hour 1 to hour 5.5 of the simulation time with 10 min sliding window.

The Fig. 1 shows how the real power of the load connected to bus 20 is varied over time. The starting point of the load variation is taken directly from the solved power flow. The figure shows only the variation profile but not the absolute load values. It can be seen that the slope is very small and the increment in the load is not significantly large. The algorithm is able to detect the change in system's operating point even when it is this small.

IV. Results

A. Illustration of the CUSUM Procedure using A Simple System

The CUSUM results are first illustrated using a small system [3] which was used in our previous work. The simulation results are shown for a simplified system with 2 modes of the minniWECC [18] selected as the poles. The change in this system is the introduction of Forced Oscillations (FO's). The total simulation time is 20 mins. The FO's are introduced at the 15th minute. The Fig. 2 show the frequency devation of the small system.

For the simple system to calculate the residue in Eq. (5), the order $p = 5$ and $q = 6$ is selected. With the chosen order numbers, the residue has a dimensionality of 5 resulting in 5 channels of decision statistics as shown in Fig. 3. Change in any channel indicates that the system has changed, and thus OR rule is used to detect the change. The residue $(\zeta(n))$ from Eq. (5) is shown in Fig. 3. The first 10 minutes are not shown here as that data is used for null space estimation for calculating the residue. For the figures presented, we see that all 5 channels show deviation from 0. In Fig. 3 it can be observed that two channels show deviation with increase in mean after the change and three channels show deviation with decrease in mean.

The CUSUM decision statistics for the test checking for an **increase** in mean is shown in Fig. 4 corresponding to Eq. (11d). Fig. 5 shows the CUSUM decision statistics for the test checking for **decrease** in mean coresponding to Eq. (12d).

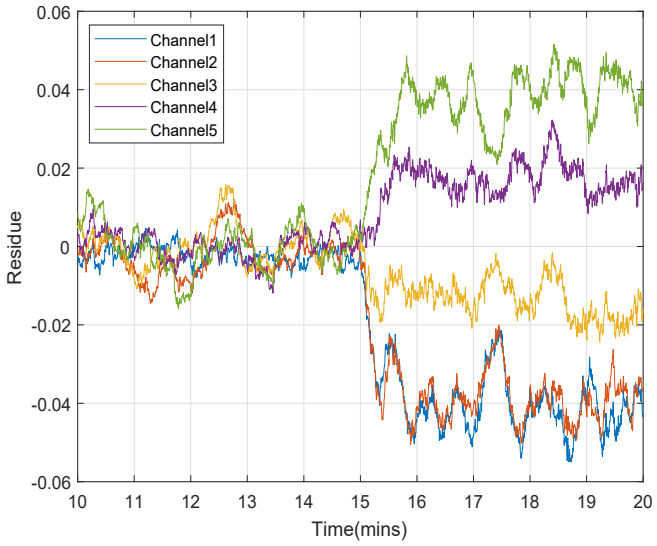

Fig. 3. The plot of residue.

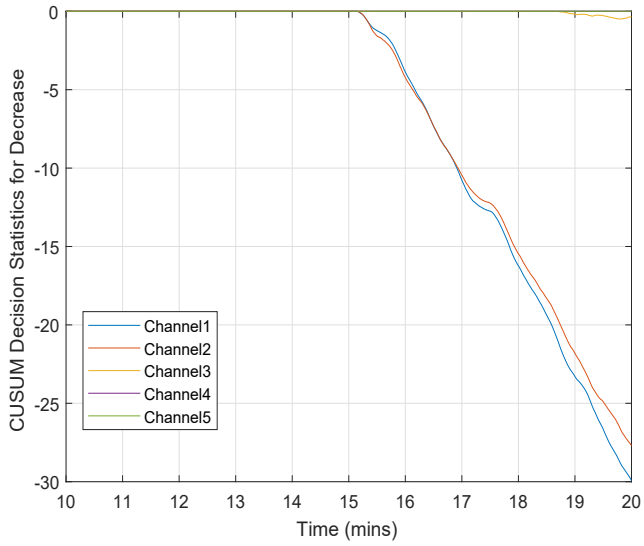

Fig. 5. The plot of g_n^- corresponding to Eq. (12d).

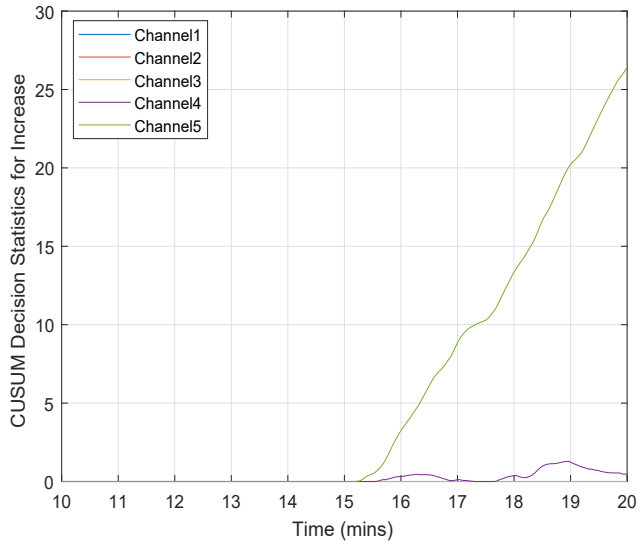

Fig. 4. The plot of g_n^+ corresponding to Eq. (11d).

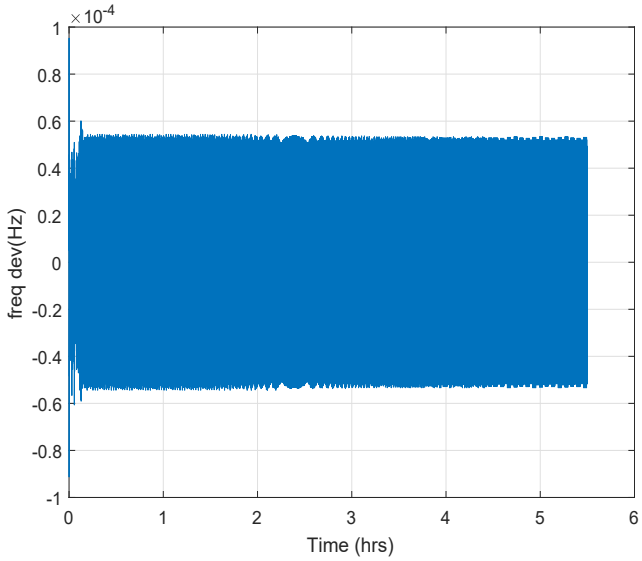

Fig. 6. The Frequency deviation between two buses of 39-bus system.

B. Hardware-in-the-Loop Testing using IEEE 39-bus System

For the hardware-in-the-loop testing, the standard IEEE 39-bus system is used. This system will have 40 channels based on the order chosen. The channel responding first, i.e., the channel that first shows deviation from 0 will be shown here since this is the used for rising the alarm with the help of the OR rule. This is done to avoid the clutter created by drawing all the 40 curves. The results presented here are of only one test of the two tests being run in parallel based on which test responded earlier.

The Fig, 6 shows the frequency deviation exhibited by the system whose nominal operating frequency is 60 Hz which is also the nominal operating frequency of the North American grid. The frequency deviation was calculated using the Eq. (18) in [2]. If the frequency deviation graph is observed it is impossible to conclude that any change is occurring in the system from 1.5 hrs to 4.5 hrs of the simulation.

Fig. 7 shows the residue corresponding to Eq. (5) from the channel which responded for the change. This figure starts at 1 hours as the algorithm is started after estimating the initial null space. The change is seen after about twenty minutes due the fact that the change in the system is very small and also the sliding window has about 10 minute memory.

Fig. 8 shows the CUSUM decision statistics corresponding to Eq. (11d) indicating the test that responded first was the one checking for **increase** in mean. Here it can be seen that there

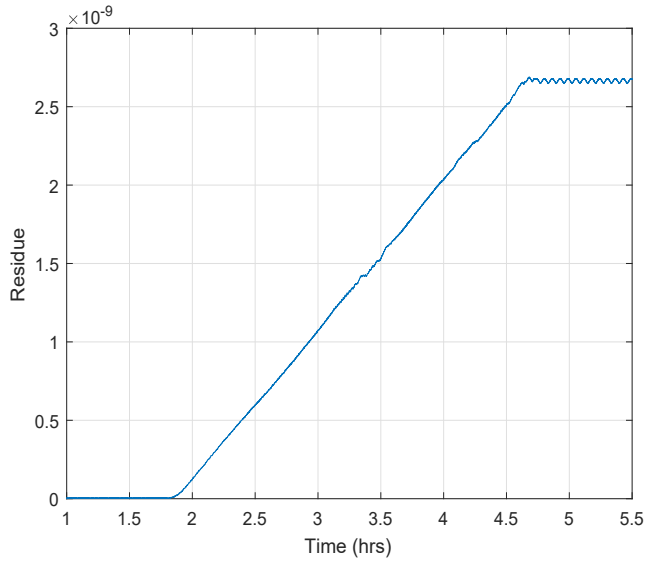

Fig. 7. The plot of residue corresponding to Eq. (5) for the channel that responded first.

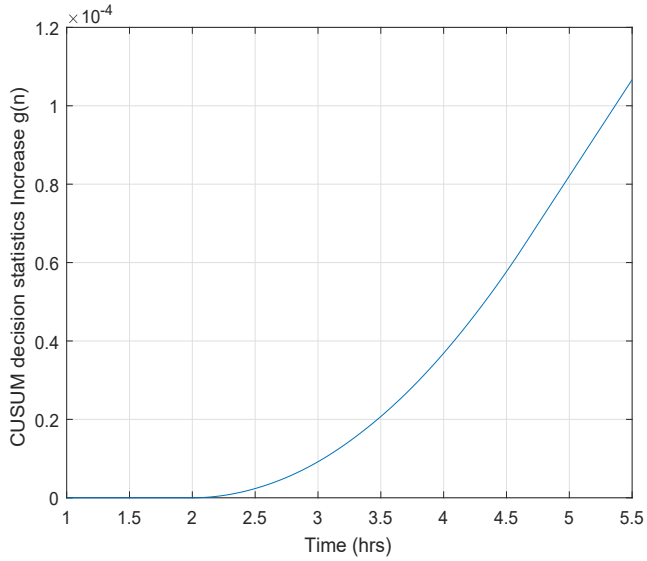

Fig. 8. The plot of g_n^+ corresponding to Eq. (11d) for the channel that responded first.

is more delay before the change is seen. This is in agreement with results of our previous work in [3], where it was shown that for having lower false alarm rate and missed detection rate, the price is paid by having a slightly higher delay of detection.

V. Conclusions

In this paper we have shown that the algorithm is able to detect the gradual or subtle changes that occur in the power system's operating point. The sudden changes in the power system's operating point were examined in our previous works [1]–[3] in detail. This work also shows that the algorithm works efficiently even with hardware-in-the-loop testing. Thus we can conclude the algorithm will be robust under varying conditions since no assumption about the system is made. The next steps would be to simulate larger system with HIL testing. The other question that needs to be answered is how to reduce the delay of detection without compromising the accuracy by designing better detection statistics and rules.

References

[1] S. Hosur and D. Duan, "Subspace-driven output-only based change-point detection of low-amplitude forced oscillations in power systems," in *2018 IEEE/PES Transmission and Distribution Conference and Exposition (T&D)*. IEEE, 2018, pp. 1–5.

[2] S. Hosur and D. Duan, "Subspace-driven output-only based change-point detection in power systems," *IEEE Transactions on Power Systems*, vol. 34, no. 2, pp. 1068–1076, 2019.

[3] S. Hosur and D. Duan, "Sequential detection of forced oscillations in power systems using the cusum procedure," in *2019 IEEE Power & Energy Society General Meeting (PESGM)*. IEEE, 2019, pp. 1–5.

[4] H. Jiang, Y. Zhang, J. J. Zhang, D. W. Gao, and E. Muljadi, "Synchrophasor-based auxiliary controller to enhance the voltage stability of a distribution system with high renewable energy penetration," *IEEE Transactions on Smart Grid*, vol. 6, no. 4, pp. 2107–2115, 2015.

[5] M. Cui, J. Zhang, C. Feng, A. R. Florita, Y. Sun, and B.-M. Hodge, "Characterizing and analyzing ramping events in wind power, solar power, load, and netload," *Renewable energy*, vol. 111, pp. 227–244, 2017.

[6] J. Li, Z. Li, F. Liu, H. Ye, X. Zhang, S. Mei, and N. Chang, "Robust coordinated transmission and generation expansion planning considering ramping requirements and construction periods," *IEEE Transactions on Power Systems*, vol. 33, no. 1, pp. 268–280, 2017.

[7] M. Aliakbari and P. Maghouli, "Mitigation of distribution system net-load ramping using multi-microgrid system," *International Transactions on Electrical Energy Systems*, vol. 30, no. 3, p. e12204, 2020.

[8] M. Bacic, "On hardware-in-the-loop simulation," in *Proceedings of the 44th IEEE Conference on Decision and Control*. IEEE, 2005, pp. 3194–3198.

[9] R. Isermann, J. Schaffnit, and S. Sinsel, "Hardware-in-the-loop simulation for the design and testing of engine-control systems," *Control Engineering Practice*, vol. 7, no. 5, pp. 643–653, 1999.

[10] H. Li, M. Steurer, K. Shi, S. Woodruff, and D. Zhang, "Development of a unified design, test, and research platform for wind energy systems based on hardware-in-the-loop real-time simulation," *IEEE Transactions on Industrial Electronics*, vol. 53, no. 4, pp. 1144–1151, 2006.

[11] J.-H. Jeon, J.-Y. Kim, H.-M. Kim, S.-K. Kim, C. Cho, J.-M. Kim, J.-B. Ahn, and K.-Y. Nam, "Development of hardware in-the-loop simulation system for testing operation and control functions of microgrid," *IEEE Transactions on Power Electronics*, vol. 25, no. 12, pp. 2919–2929, 2010.

[12] O. Crăciun, A. Florescu, S. Bacha, I. Munteanu, and A. I. Bratcu, "Hardware-in-the-loop testing of pv control systems using rt-lab simulator," in *Proceedings of 14th International Power Electronics and Motion Control Conference EPE-PEMC 2010*. IEEE, 2010, pp. S2–1.

[13] P. Kotsampopoulos, D. Lagos, N. Hatziargyriou, M. O. Faruque, G. Lauss, O. Nzimako, P. Forsyth, M. Steurer, F. Ponci, A. Monti *et al.*, "A benchmark system for hardware-in-the-loop testing of distributed energy resources," *IEEE Power and Energy Technology Systems Journal*, vol. 5, no. 3, pp. 94–103, 2018.

[14] R. Zouari, L. Mevel, and M. Basseville, "Adaptive statistical approach to flutter detection," *Journal of Aircraft*, vol. 49, no. 3, pp. 735–748, 2012.

[15] M. Basseville, A. Benveniste, M. Goursat, and L. Meve, "In-flight vibration monitoring of aeronautical structures," *IEEE Control Systems*, vol. 27, no. 5, pp. 27–42, 2007.

[16] M. Basseville, "Detecting changes in signals and systems — a survey," *Automatica*, vol. 24, no. 3, pp. 309–326, 1988.

[17] L. Mevel, M. Basseville, and A. Benveniste, "Fast in-flight detection of flutter onset: a statistical approach," *Journal of guidance, control, and dynamics*, vol. 28, no. 3, pp. 431–438, 2005.

[18] D. Trudnowski and J. Undrill, "The minniwecc system model," *Oscillation damping controls*, 2008.